

# Power System Stability Investigation Using Micro Grid

**Abinash Singh\* and Balwinder Singh Surjan**

Electrical Engineering Department, Punjab Engineering College (Deemed to be University)  
Chandigarh –160012, India  
✉ abinashsinghphd@gmail.com

*Received March 8, 2018; revised and accepted April 13, 2018*

**Abstract:** This paper presents the MATLAB simulation and stability investigation of a power system in the presence of micro grid. Micro grid considered has hydro, wind and PV energy sources as its constituents. Different possible combinations of these energy sources have been presented and the system response is analysed. Fuzzy logic controller has also been incorporated in the rotor side and grid side converters of DFIG of wind power plant. The effect of micro grid on the system during grid connected and partially islanded modes is investigated through voltage, current, power and frequency. The system performance under different combinations of the micro grid constituents has been studied using ISE performance index.

**Key words:** Micro grid, distributed power generation, renewable energy source, DFIG, photovoltaic systems.

## Introduction

The depletion of fossil fuels and global energy consumption has increased at a fast pace. For the improvement in energy utilization, reliability and to cope up with the increasingly growing demand of electricity, new power generation technologies, such as renewable energy, clean and efficient sources have been incorporated (Özbay and Tunay, 2010; Singh and Surjan, 2014; Ozdemir et al., 2012).

Nithya and Ramasamy (2014) found that there are numerous applications demanding higher reliability and availability of electrical power, which has been obtained through the arrangement of multiple power sources. Renewable Energy Sources (RES) have also been installed in off-grid rural electrification (Barall et al., 2012).

Ananda Kumar et al. (2012) described Distributed Generation (DG) as combination of renewable energy sources at distribution level. RES will never expire as they are constantly replenished. Vast markets for the

application of renewable energy technologies are the islands and also for the global campaign of renewable energy. Nayar et al. (2008) reported that one of the most lavish and environmentally unfavourable ways of generating electricity is with the usage of diesel. It becomes vital to ponder for unconventional renewable resources such as wind, solar, hydro etc. due to environmental pollution and extreme heat production through the combustion of non-renewable fuels (Singh et al., 2012).

Renewable Energy Sources (RES) using power electronic converters have been progressively coupled in the distribution systems to meet the growing load demand. In order to preserve the reliability and quality of power-supply, new approaches are required for proper operation of power grid (Suresh and Srinivas, 2013). The power system performance can be gradually improved by the growing number of renewable energy sources along with grid linked energy storage devices (Tenti et al., 2010).

The concept of Micro Grid (MG) has been suggested

\*Corresponding Author



as operational way out for weak power systems, like the rural areas as they are distant from the main grid network. When surplus/deficit of power occurs in the MG, power exchange is also possible with the main grid (Arulampalam et al., 2010; Chukka et al., 2014). With incorporation of intelligent control techniques, the interconnection of wind energy systems and solar power plants, the electric grids have become smarter (Abo et al., 2012).

RES are irregular in nature so perception of future network technologies comprising Micro Grid technology using renewables interfaced with alternative energy sources such as fuel cells, joined with power electronic system, and energy storage devices, are being shaped (Nithya and Ramasamy, 2014; Khamis et al., 2013; Dhivya and Dhamodharan, 2013).

The paper comprises a brief introduction of Micro Grid, description of the test system and the modelling of the micro grid comprising combinations of hydro, wind (DFIG) and photovoltaic (PV) system; the responses of the test system are obtained and inferences are drawn.

### Mathematical Modelling

The Micro Grid (MG) comprises Distributed Energy Resources (DERs) comprising diesel generators, renewable energy sources, to cope up with the desired load demand and maintaining system stability and reliability whether operated in grid-connected mode or stand-alone (Kim et al., 2015; Syed et al., 2013; Honarmand et al., 2014).

#### Hydro Energy Source

The synchronous machine's mathematical model can be represented in  $d$ - $q$  reference frame from equations as given below:

$$V_d = \frac{d}{dt}\phi_d + i_d R_s - \omega_R \phi_q \quad (1)$$

$$V_q = \frac{d}{dt}\phi_q + i_q R_s + \omega_R \phi_d \quad (2)$$

$$V'_{kd} = \frac{d}{dt}\phi'_{kd} + i'_{kd} R'_{kd} \quad (3)$$

$$V'_{kd1} = \frac{d}{dt}\phi'_{kd1} + i'_{kd1} R'_{kd1} \quad (4)$$

$$V'_{kd2} = \frac{d}{dt}\phi'_{kd2} + i'_{kd2} R'_{kd2} \quad (5)$$

$$V'_{fd} = \frac{d}{dt}\phi'_{fd} + i'_{fd} R'_{fd} \quad (6)$$

$$T_e = \phi_d i_q - \phi_q i_d \quad (7)$$

$$\frac{d}{dt}\omega_m = \frac{P}{2H_m}(T_m - T_e) \quad (8)$$

where

$$T_m = \frac{1}{\omega_m} \rho g \eta H Q \quad (9)$$

The parameters in above equations are referred to stator in which suffixes 'R' denotes rotor parameter, 's' denoting stator parameter, 'p' is number of poles (Kulkarni and Thosar, 2013).

Small Hydro Plant (SHP) can be modelled along with adaptive fuzzy logic controllers (Özbay and Tunay, 2010; Ozdemir and Orhan, 2012; Barall et al., 2012). The synchronous generator and its excitation system can be mathematically modelled as below.

Output power of a hydro plant is expressed as below:

$$P = \rho g \eta H Q \quad (10)$$

In the above equation the mechanical power output at the turbine shaft is equal to the product of the water density ( $\rho$ ), the gravitational acceleration ( $g$ ), the turbine's hydraulic efficiency ( $\eta$ ), water head ( $H$ ), and the water flow rate through the turbine ( $Q$ ). Power at the turbine wheel is:

$$P = 3.74 \times 10^{-6} \times (q \times v^2) \text{ kW} \quad (11)$$

where  $q$  is volumetric flow rate (L/min) and  $v$  is nozzle velocity (m/s).

Basic concept which has been used in this study to model the hydropower plant in MATLAB/Simulink is presented in Figure 1.

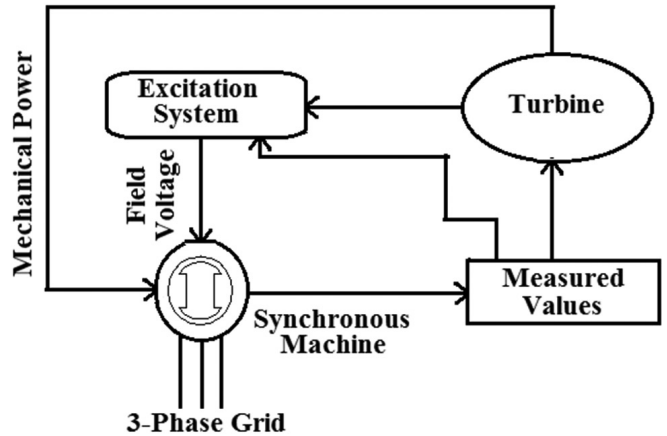


Figure 1: Layout of hydropower plant.



### Wind Energy Source

Doubly-Fed Induction Generator (DFIG) can be mathematically modelled as given below.

*Electrical system:*

$$V_{qs} = \frac{d}{dt} \phi_{qs} + R_s i_{qs} + \omega \phi_{ds} \quad (12)$$

$$V_{ds} = \frac{d}{dt} \phi_{ds} + R_s i_{ds} - \omega \phi_{qs} \quad (13)$$

$$V'_{qr} = \frac{d}{dt} \phi'_{qr} + R'_r i'_{qr} + (\omega - \omega_r) \phi'_{dr} \quad (14)$$

$$V'_{dr} = \frac{d}{dt} \phi'_{dr} + R'_r i'_{dr} - (\omega - \omega_r) \phi'_{qr} \quad (15)$$

$$T_e = 1.5p(\phi_{ds} i_{qs} - \phi_{qs} i_{ds}) \quad (16)$$

The above equations are referred to the stator. The rotor and stator quantities are in the  $d$ - $q$  reference frame (Sarker et al., 2014; Boulâam and Boukhefifa, 2014).

*Mechanical equation of wind energy system:*

$$T_m = \frac{P_m}{\omega_m} \quad (17)$$

$$\frac{d}{dt} \omega_m = \frac{1}{2H_m} (T_m - T_e) \quad (18)$$

$$\frac{d}{dt} \theta_m = \omega_m \quad (19)$$

where  $P_m$  is the wind turbine's power output and is presented by the following equation:

$$P_m = v_{wind}^3 (\rho A / 2) C_p(\lambda, \beta) \quad (20)$$

in which, ' $v_{wind}$ ' is the wind speed in (m/s), ' $\rho$ ' symbolizes the air density, pitch angle of the blade is defined by ' $\beta$ ', turbine swept area is ' $A$ ' in  $m^2$ , and ' $\lambda$ ' is the tip speed ratio,  $C_p$  = power coefficient.

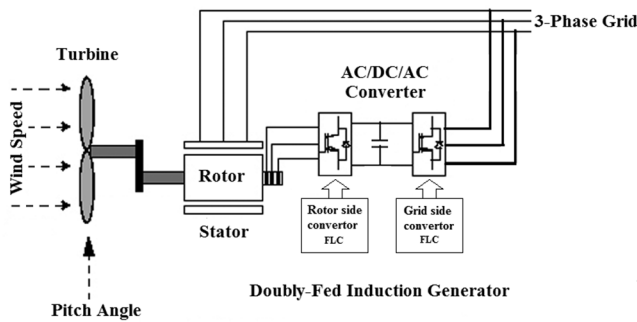


Figure 2: Wind power plant with DFIG.

DFIG is shown in Figure 2, in which wind turbine is connected to DFIG and has two input parameters – wind speed and pitch angle. There are two converters being used, one on rotor side and other on grid side for AC/DC/AC conversion and at last the DFIG is linked to the three-phase grid.

### Solar Energy Source

Mature micro grid systems containing PV system have been presented as in (Nayar et al., 2008 and Arulampalam et al., 2010). PV systems are becoming integral part of latest micro grids. Intelligent control techniques make the micro grids more smarter (Abo et al., 2012). As a whole the solar cells, protective parts and supports is known as photovoltaic (PV) module (Singh et al., 2012).

$I$  is the current output of a solar cell as follows

$$I = (I_{sg} \times I_{rad} / I_{r0}) - (V + I \times R_s) / R_p - I_d \times (e^{(V+I \times R_s)/(N \times V_t)} - 1) \quad (21)$$

where  $I_{rad}$  is the irradiance falling on the cell.  $I_{sg}$  is the solar-generated current.  $I_d$  is saturation current for the diode and thermal voltage is expressed by  $V_t$ .  $N$  is quality factor for the diode. And at last the voltage across the electrical ports of solar cell is represented by  $V$ .

PV module is connected to three-phase AC grid via DC to AC converter as shown in Figure 3.

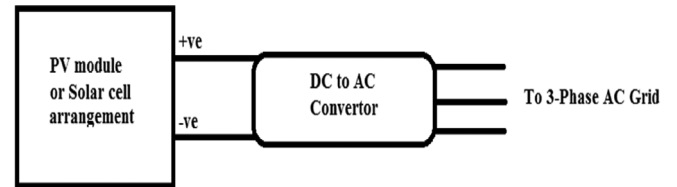


Figure 3: PV module interfaced to 3-phase AC grid.

### Fuzzy Logic Controller

As shown in Figure 4, a Fuzzy Logic Controller (FLC) comprises: (i) fuzzification, (ii) rule base, (iii) inference mechanism and (iv) defuzzification. The fuzzification includes processing the inputs into fuzzy values with trapezoid, triangle or other appropriate forms of membership functions. One can form the rule base by experimenting or by hit and trial method. The rule base contains if-then rules which are used by an inference engine to obtain the output. After that the defuzzification process transforms the output from the inference tool into the crisp values (Özbay and Tunay,



2010; Ozdemir and Orhan, 2012; Ananda Kumar and Srinivasa Rao, 2012).

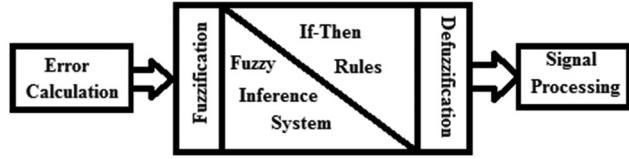


Figure 4: Fuzzy logic controller.

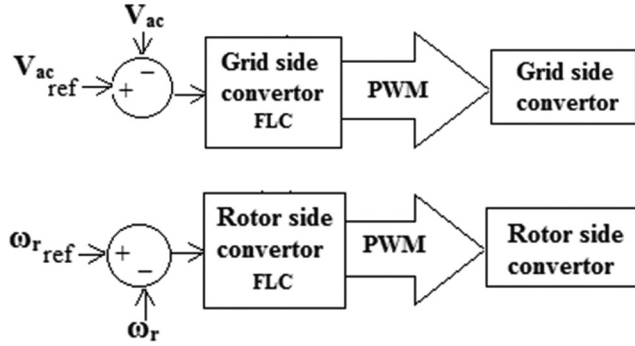


Figure 5: Fuzzy logic controller in DFIG.

As shown in Figure 5, FLC has been used in this study to control grid side converter and the rotor side converter of DFIG in wind system, using 49 fuzzy rules. During grid side converter control, grid side AC voltage  $V_{ac}$  is the control parameter. While in rotor side converter the rotor speed  $\omega_r$  is used as control parameter.

### Test System and Performance Index

The system being tested in this paper has a 0.4 KV three-phase supply and has two permanent connected

loads of 75 KW each as shown in Figure 6. Different combinations of the renewable energy sources have been tried to form micro grid and producing power at 400 V voltage level which is connected to main voltage line.

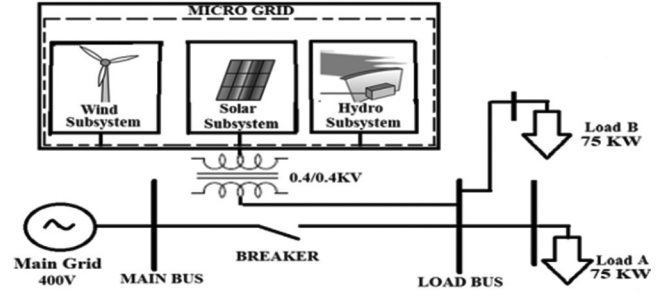


Figure 6: Test system embedded with micro grid.

The MATLAB/SIMULINK model for the test system embedded with Microgrid is presented in Figure 7. The simulation results have been obtained through for two modes: fully grid connected mode and partially islanded mode.

There are many renewable energy sources available but the major sources under consideration in this paper are: hydro, wind and solar energy sources. Circuit breaker is used to isolate the load bus from main grid and thus switching from grid connected mode to islanded mode and vice-versa.

### Different Cases under Consideration for Mode I: Grid-Connected

*Case 1:* Base system without micro grid.

*Case 2:* System with micro grid having hydro and solar energy sources.

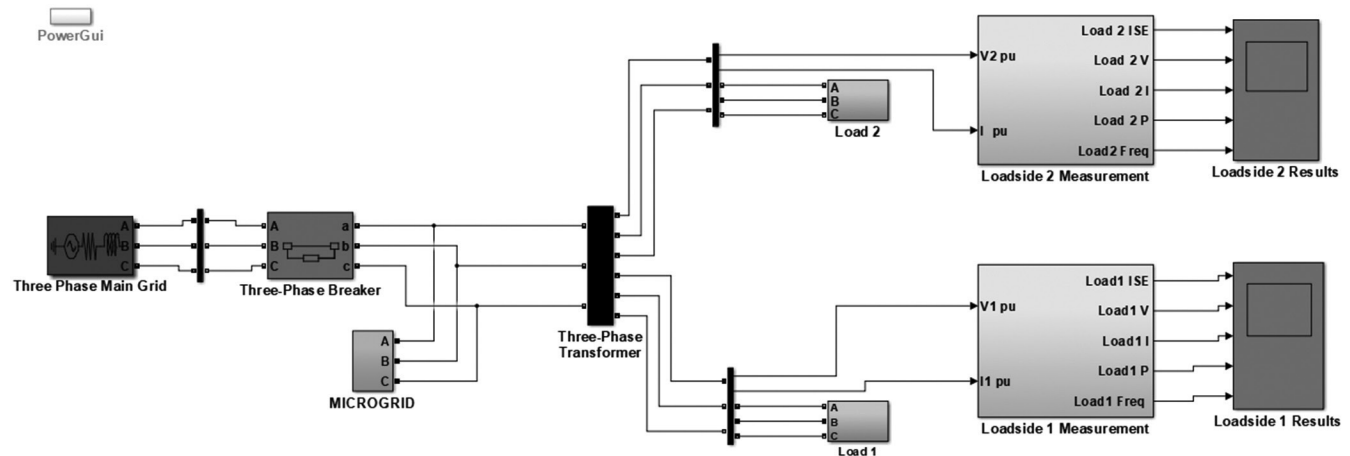


Figure 7: SIMULINK model of test system embedded with Microgrid.



*Case 3:* System with micro grid having hydro and wind energy sources.

*Case 4:* System with micro grid having solar and wind energy sources.

*Case 5:* System with micro grid having hydro, solar and wind energy sources.

### Different Cases under Consideration for Mode II: Islanded

*Case 1:* Base islanded system without micro grid.

*Case 2:* Islanded system with micro grid having hydro and solar energy sources.

*Case 3:* Islanded system with micro grid having hydro and wind energy sources.

*Case 4:* Islanded system with micro grid having solar and wind energy sources.

*Case 5:* Islanded system with micro grid having hydro, solar and wind energy sources.

### Performance Index

ISE performance index is a process to measure or judge the system performance by estimating the parameters (Soni and Bhatt, 2013; Kishnani et al., 2014) and is expressed as below:

$$ISE = \int_0^{\infty} e^2(t) dt \quad (22)$$

where 'e' is the error in loadside voltage in the present investigation.

## Results and Discussion

The impact of micro grid on the load side has been presented and analysed through voltage, current, power, frequency and ISE. As both the loads are identical and the results obtained on both loadsides are same. The results across one loadside are presented only. The base test system has been simulated and its results are taken as reference values and compared with other combinational results.

### Mode I: Grid Connected Mode

The simulation is run for two seconds and breaker is in closed position for whole duration to ensure the grid connection. Following results are obtained for this mode.

#### Load Side Voltage

The voltage value is 1 p.u in base test system and that is taken as reference value for rest of cases. From the simulation results, it has been observed that for different combinations of considered renewable energy sources connected to the system under different cases, there is no applicable change in load side voltage and always close to 1 p.u as presented in Figure 8.

#### Load Side Current

While analyzing the source side current from the results shown in Figure 9, it has been found that the current waveform is without any variations and its magnitude is balanced throughout near 1 p.u (reference value of base test system) in all cases except the combinations involving wind energy source, in which current is slightly on higher side due to additional supplied power.

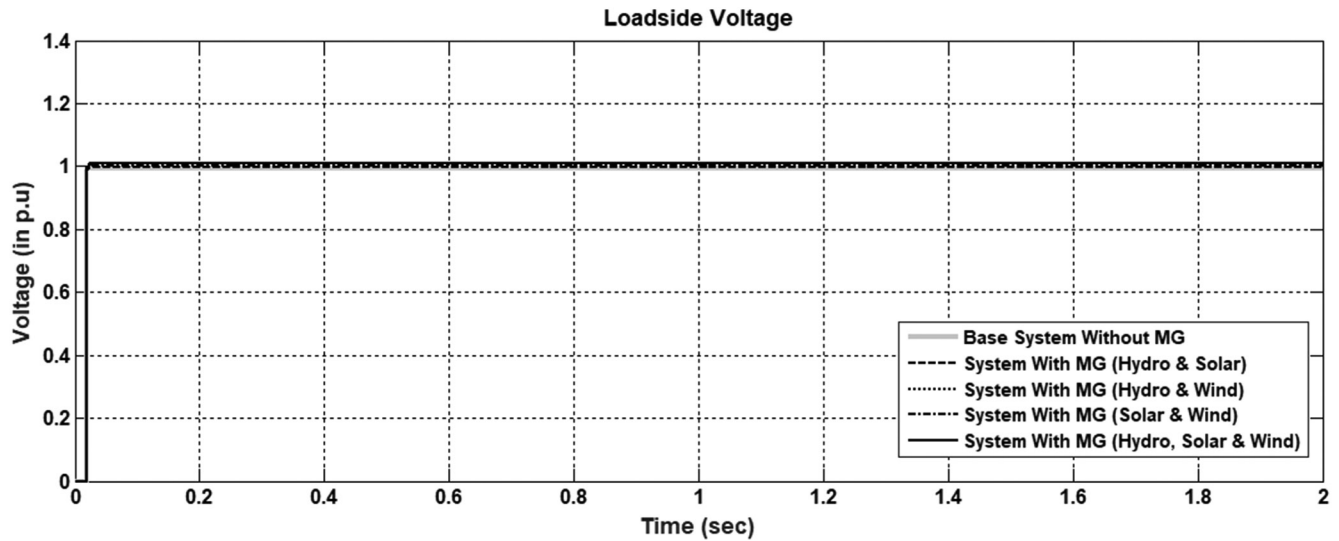


Figure 8: Load side voltage for systems in grid-connected mode with and without MG.



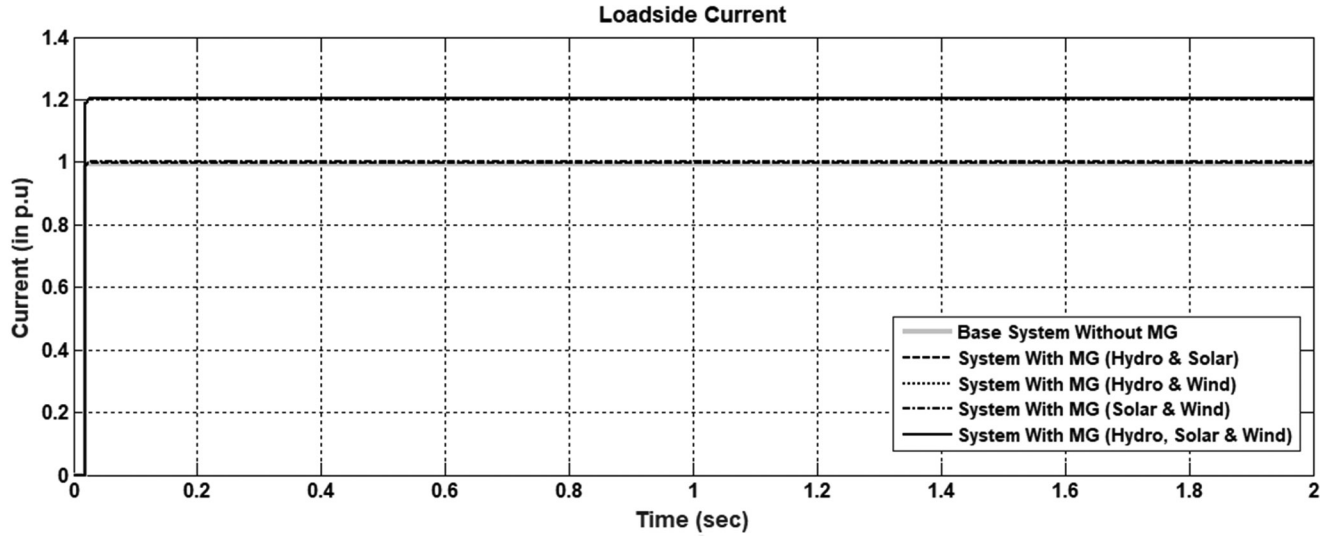


Figure 9: Load side current for systems in grid-connected mode with and without MG.

#### Load Side Power

During the study of the MG's impact on load side, the active power has also been analysed as shown in Figure 10. For all the system combinations the active power have very small initial variations for fraction of initial seconds but get stable afterwards in each case. Here in this study, the power presented is near 1.5 p.u for base reference test system. In most cases the value remains closer to that reference value but when wind energy source is part of microgrid combination, there is additional increase in power.

#### Load Side Frequency

Upon analysing the load side frequency waveforms for five different cases as shown in Figure 11, it can be seen that in all cases frequency attains stability at 50

Hz quite well while some detailed observations were made as given in Table 1.

Table 1: Variations in load side frequency (for Mode I)

Case system	Highest value of frequency	Lowest value of frequency
Base system without MG	50.034	49.906
System with MG (hydro & solar)	50.034	49.904
System with MG (hydro & wind)	50.025	49.939
System with MG (wind & solar)	50.026	49.929
System with MG (hydro, wind & solar)	50.026	49.930

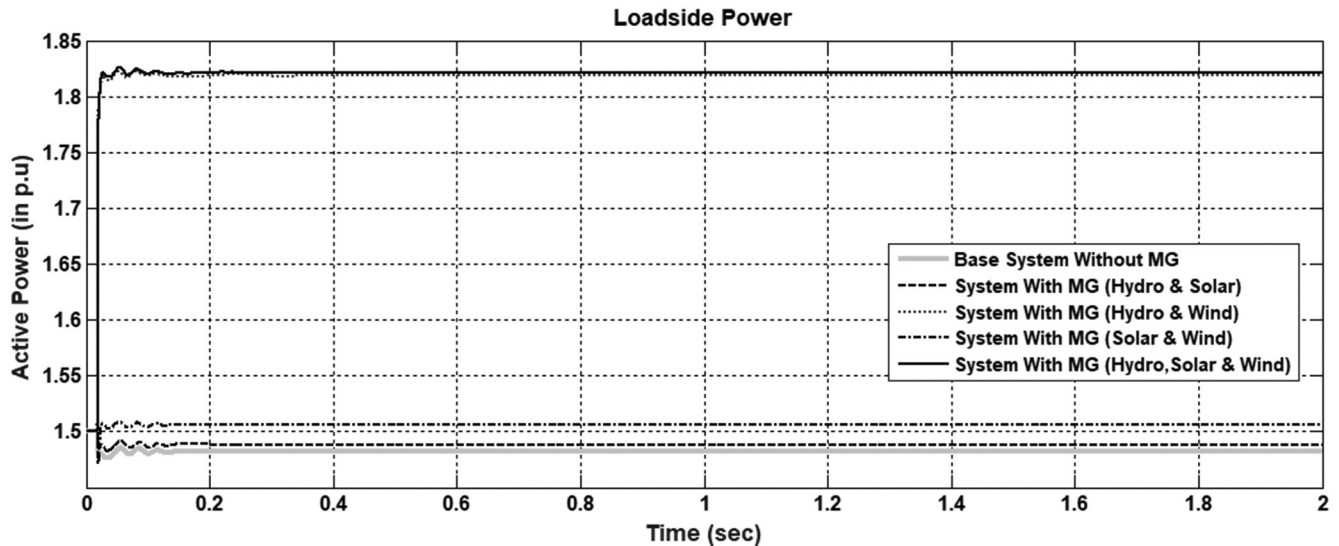


Figure 10: Load side active power for systems in grid-connected mode with and without MG.



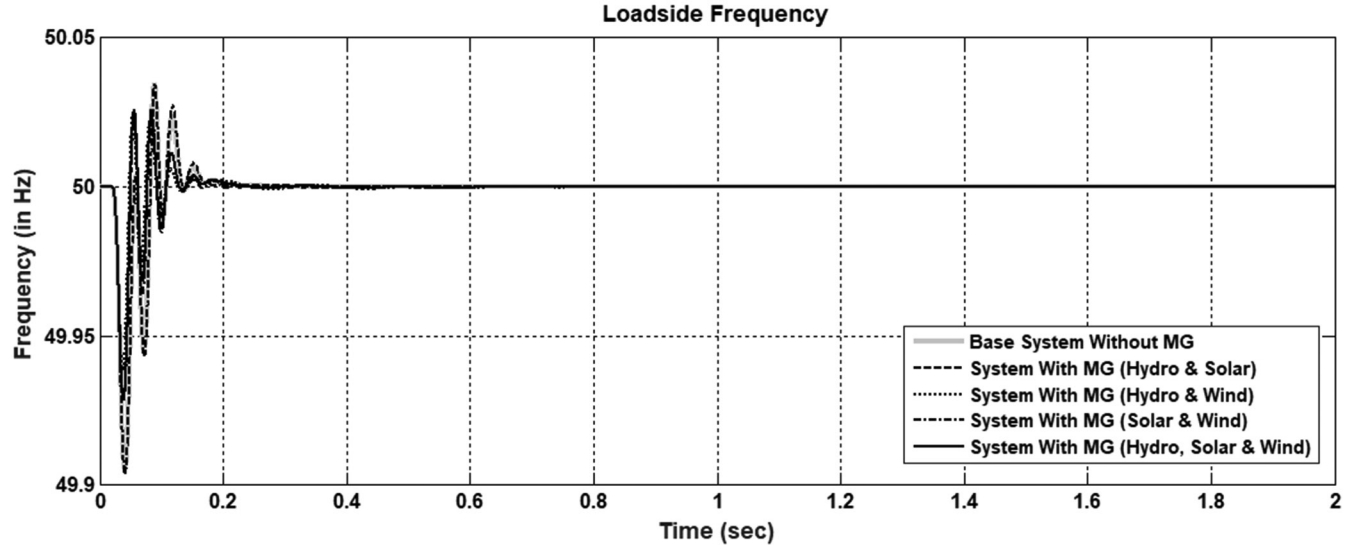


Figure 11: Load side frequency for systems in grid-connected mode with and without MG.

#### Load Side ISE

The ISE for all five cases are given in Figure 12, where it has been observed that the ISE value for system with MG has increased as compared to the value for basic system as shown in Table 2.

Table 2: Variations in load side ISE (for Mode I)

Case System	ISE value
Base system without MG	0.02000
System with MG (hydro & solar)	0.02003
System with MG (hydro & wind)	0.02017
System with MG (wind & solar)	0.02001
System with MG (hydro, wind & solar)	0.02019

#### Mode II: Partially Islanded Mode

The simulation is run for four seconds and breaker is made to open for brief time period i.e. 1.1 to 2.5 sec so as to make the loadside islanded from main grid and for rest of time breaker is in closed position for the grid connection. Following results are obtained for this mode.

#### Load Side Voltage

From the simulation results obtained for load side voltage, it can be seen there is voltage outage during the islanded mode i.e. from 1.1 sec to 2.5 sec for the case of islanded system without any micro grid as compared to the base non-islanded system. For the system without MG, there is voltage outage for the

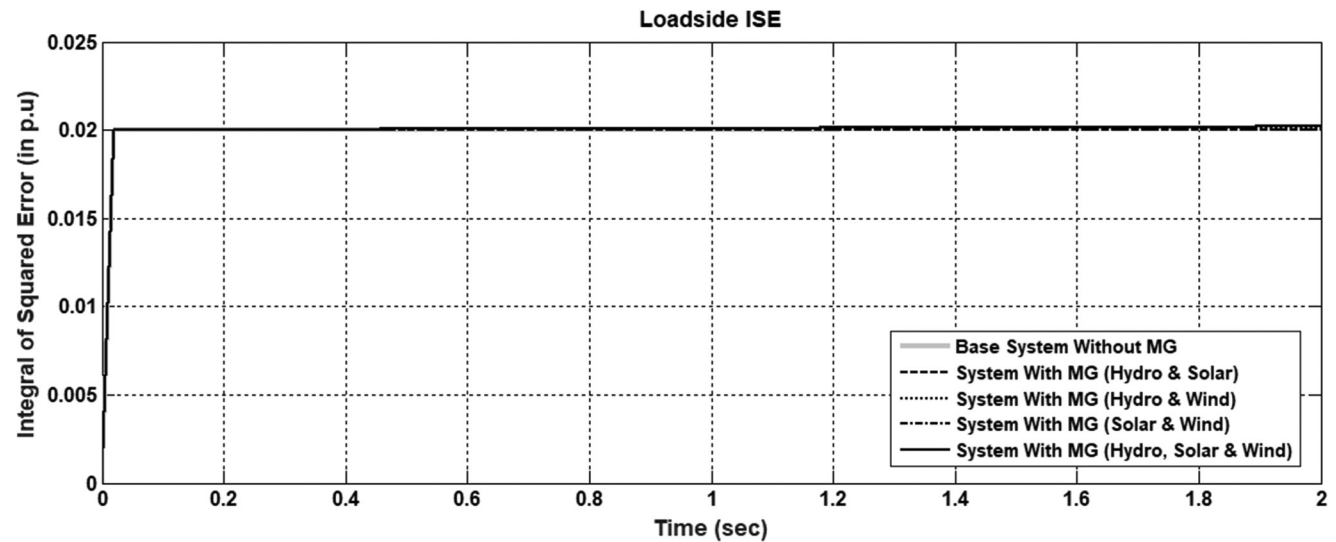


Figure 12: Load side ISE for systems in grid-connected mode with and without MG.



period of islanded mode. It has been observed that for different combinations of renewable energy sources connected to the system, there is considerably good voltage restoration done. It can be seen in Figure 13 that there are small variations in voltage for all cases of micro grid during switching of circuit breaker.

#### Load Side Current

The simulation results obtained for load side current for base system and different cases of combinations of MG with system were obtained (as shown in Figure 14), from which it has been analyzed that there is almost similar drop in value of current as it has been observed in voltage but the value of current magnitude goes more than 1 p.u in multiple cases while it tries to stay at 1 p.u in two cases involving solar energy source.

#### Load Side Power

Simulation results of load side power for different combination cases of MG connected to the system have been presented in Figure 15. In comparison with waveform for base system, it is found that value for power has been restored to close to the expected value for different combinations of MG during islanded mode whereas the system without MG fails to supply power when switched to islanded mode.

#### Load Side Frequency

Load side frequency response for different cases during islanded mode have been shown in Figure 16 and it can be seen that the system without MG loses its synchronism once switched to islanded mode and its frequency falls at faster rate and further analysis has been made as shown in Table 3.

**Table 3: Variations in load side frequency (for Mode II)**

Case	Highest value of frequency	Lowest value of frequency
Base islanded system without MG	50.0	49.25
Islanded system with MG (hydro & solar)	50.2	49.87
Islanded system with MG (hydro & wind)	50.3	49.65
Islanded system with MG (wind & solar)	50.2	49.80
Islanded system with MG (hydro, wind & solar)	50.2	49.80

#### Load Side ISE

ISE for cases consisting system with and without MG combinations has been compared as examined in Figure 17 and also given in Table 4.

**Table 4: Variations in load side ISE (for Mode II)**

Case system	ISE value
Base islanded system without MG	1.41
Islanded system with MG (hydro & solar)	0.02041
Islanded system with MG (hydro & wind)	0.02582
Islanded system with MG (wind & solar)	0.02329
Islanded system with MG (hydro, wind & solar)	0.02047

During islanded mode ISE of system without MG rises to 1.41 from base value of 0.02. System with different MG combinations tried to bring that value close to reference value of base system i.e. 0.02.

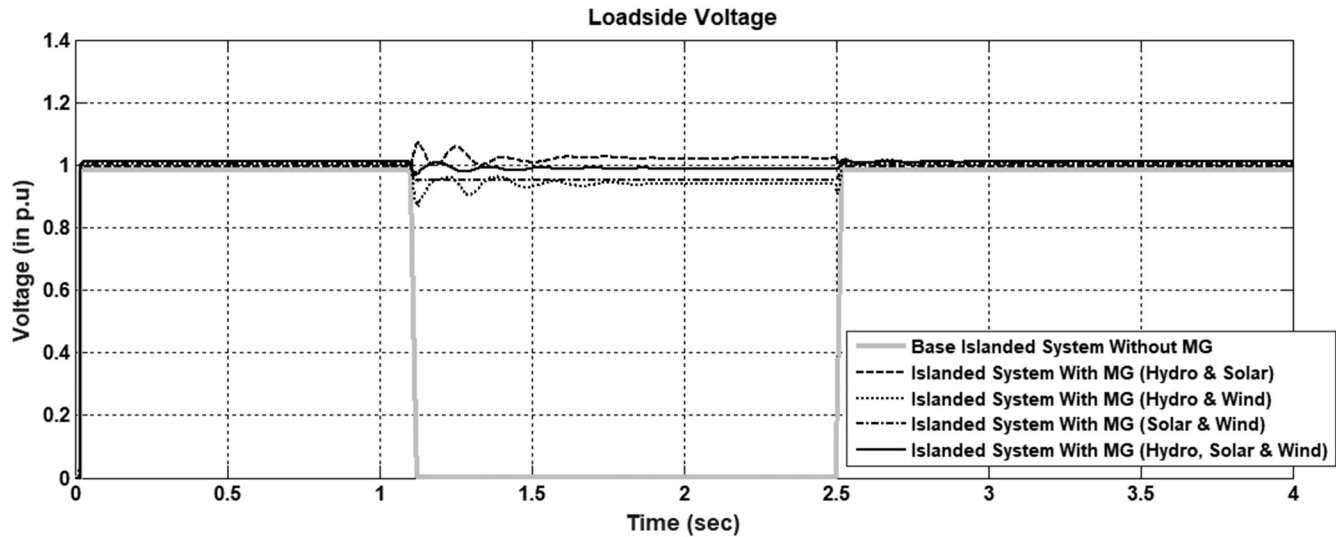


**Figure 13: Load side voltage for systems in partially-islanded mode with and without MG.**



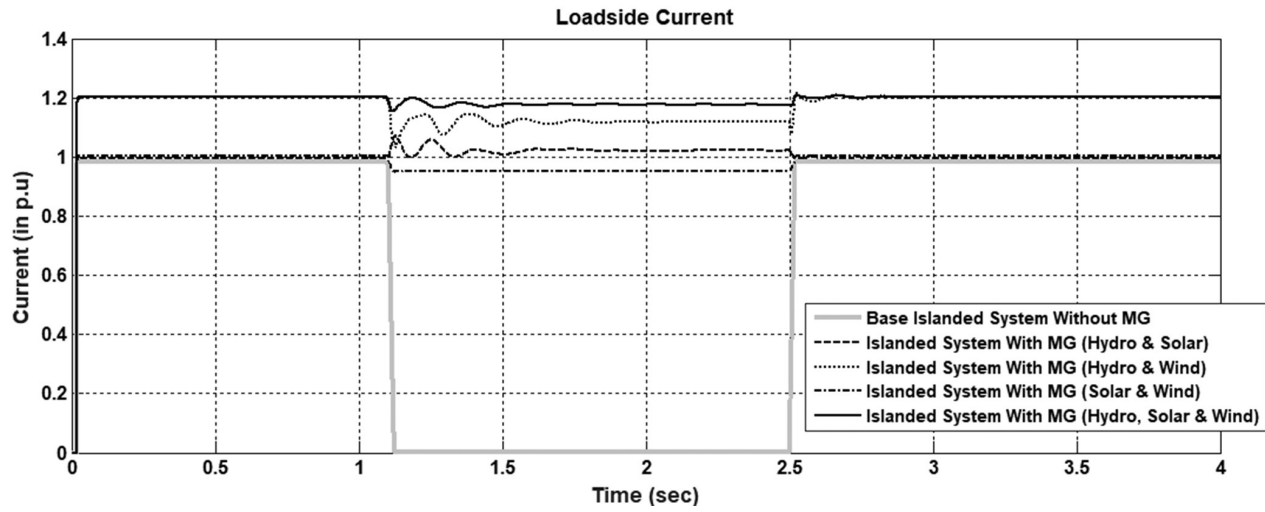


Figure 14: Load side current for systems in partially-islanded mode with and without MG.

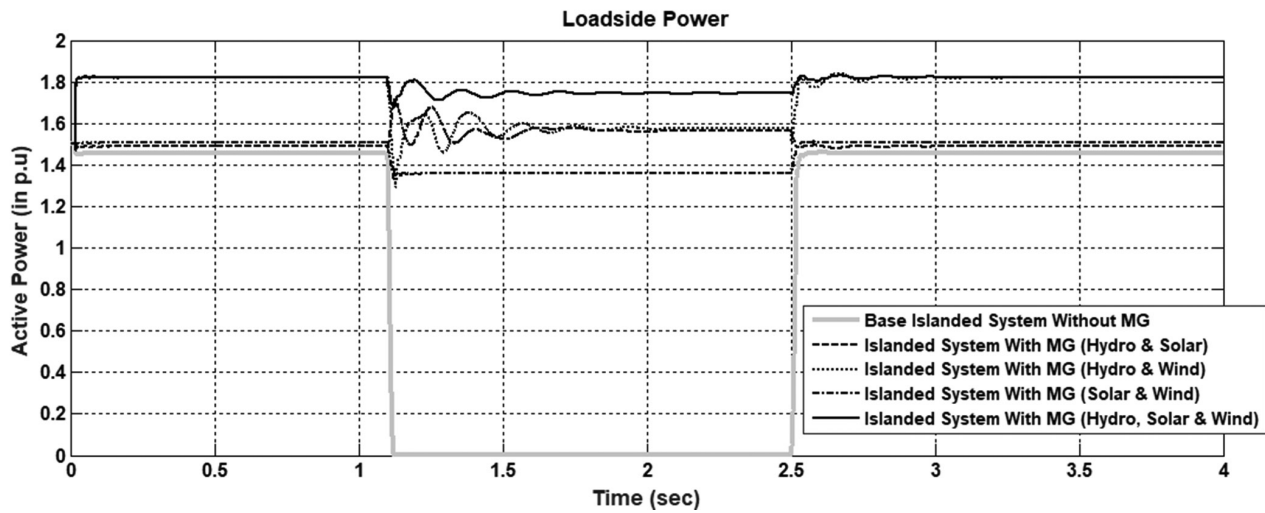


Figure 15: Load side active power for systems in partially-islanded mode with and without MG.

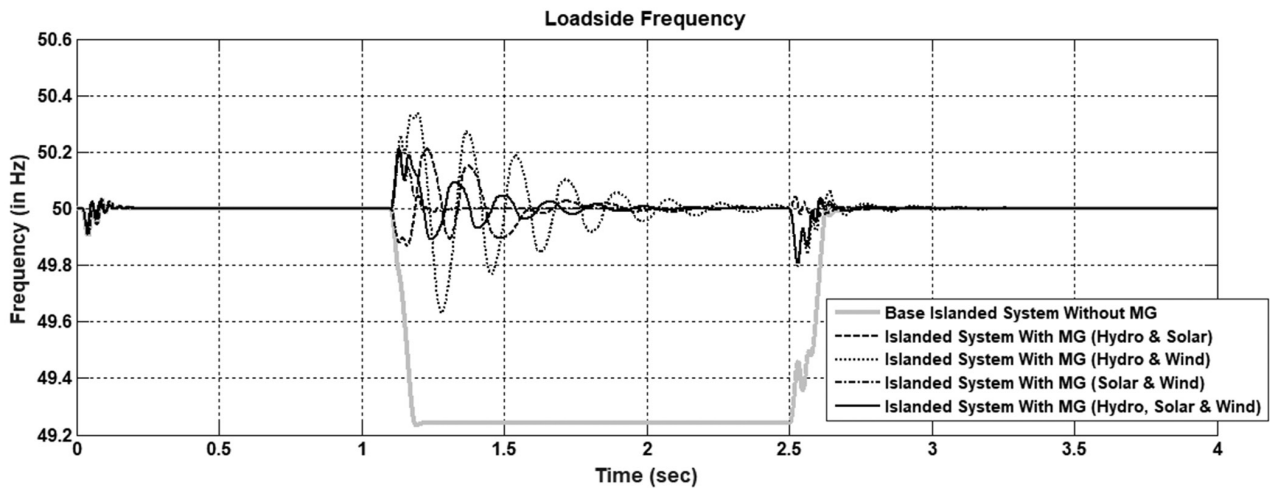


Figure 16: Load side frequency for systems in partially-islanded mode with and without MG.



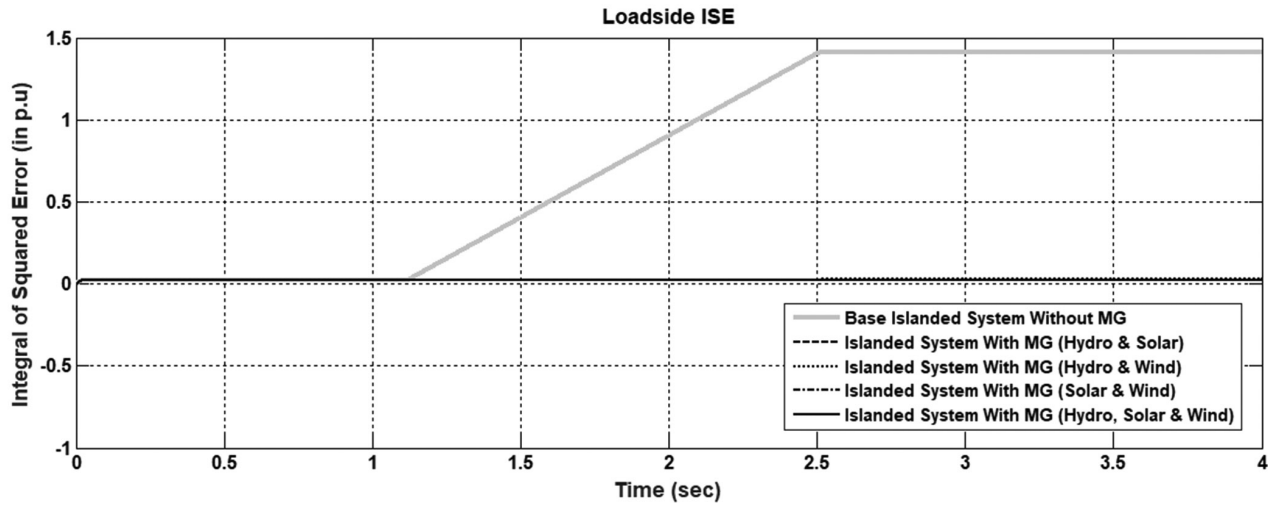


Figure 17: Load side ISE for systems in partially-islanded mode with and without MG.

### Hydro Subsystem Rotor Speed and Wind Subsystem DFIG Rotor Speed

The response of hydro subsystem and wind subsystem with respect to their rotor speed have been presented in Figures 18 and 19. The rotor speed in hydro subsystem first varies in initial stage and attains steady state at 1 p.u., whereas DFIG rotor speed increases gradually and stabilizes at 1 p.u.

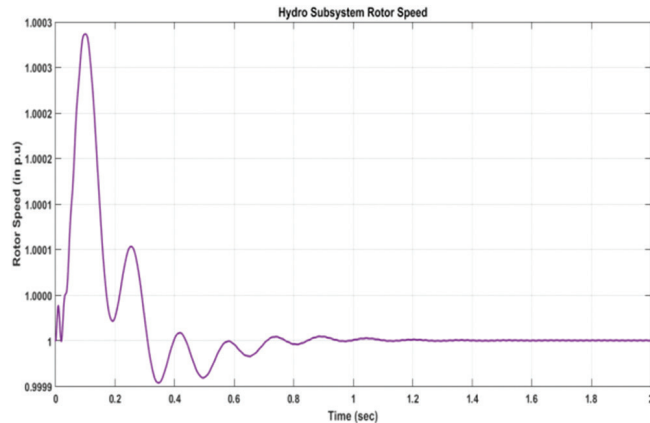


Figure 18: Hydro subsystem rotor speed for the system with MG having hydro energy source.

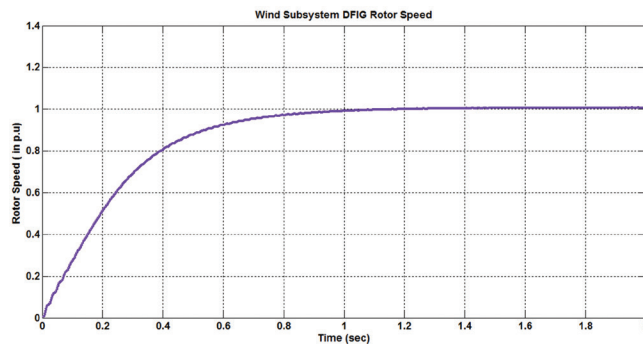


Figure 19: Wind subsystem DFIG rotor speed for the system with MG having wind energy source.

### Conclusion

The renewable energy sources in a combined form makes micro grid which can be connected to the power system. The impact of micro grid has been observed through voltage, current, power and frequency. The system response in the presence of different combinations of MG constituents in the system has been compared to the response of base system and analyzed during fully grid connected and partially islanded modes. The presence of MG helps in restoring the voltage supply during islanded mode with minimum impact on system during grid connection which is justified from values of the performance index and also helps in maintaining power quality.

### References

- Abo-Al-Ez, K.M., Xia, X. and J. Zhang (2012). Smart Interconnection of a PV/Wind Dg Micro Grid with the utility distribution network. IEEE Industrial and Commercial Use of Energy Conference, 1-8.
- Ananda Kumar, A. and J. Srinivasa Rao (2012). Power Quality Improvement of Grid Interconnected 3-phase 4-wire Distribution System using Fuzzy logic control. *International Journal of Engineering Research & Technology*, 1-4: 1-5.
- Arulampalam, N. Mithulananthan, Bansal, R.C. and T.K. Saba (2010). Micro-grid Control of PV-Wind-Diesel Hybrid System with Islanded and Grid Connected Operations. IEEE International Conference Sustainable Energy Technologies.
- Barall, S., Budhathoki, S. and H. Neopane (2012). Grid connection of Micro Hydropower, Mini Grid initiatives



- and rural electrification policy in Nepal. IEEE International Conference Sustainable Energy Technologies, 66-72.
- Boulâam, K. and A. Boukhelifa (2014). Fuzzy Sliding Mode Control of DFIG Power for a Wind Conversion System. IEEE International Power Electronics and Motion Control Conference and Exposition, 353-358.
- Chukka, G., Pinninti, S. and P. Venkatesh (2014). Modeling and Simulation of Microgrid Connected Renewable Energy Resources with MPPT Controller and by Using SVPWM Technique. *International Journal of Engineering Research & Technology*, **3-1**: 455-462.
- Dhivya, B. and S. Dhamodharan (2013). Analysis of multiport DC-DC converter in Renewable Energy Sources. *International Journal of Research in Engineering and Technology*, **02-10**: 181-184.
- Honarmand, M., Zakariazadeh, A. and S. Jadid (2014). Integrated scheduling of renewable generation and electric vehicles parking lot in a smart microgrid. *International Journal of Energy Conversion and Management*, **86**: 745-755.
- Khamis, A. Mohamed, H. Shareef and A. Ayob (2013). Modeling and simulation of a Microgrid testbed using Photovoltaic and Battery based power generation. IEEE European Modelling Symposium.
- Kim, G., Hwang, C., Jeon, J., Ahn, J. and E. Kim (2015). A novel three-phase four-leg inverter based load unbalance compensator for stand-alone microgrid. IEEE International Conference on Power Electronics and ECCE Asia, 1491-1496.
- Kishnani, M., Pareek, S. and R. Gupta (2014). Comparison of Different Performance Index Factor for ABC-PID Controller. *International Journal of Electronic and Electrical Engineering*, **7-2**: 177-182.
- Kulkarni, S.S. and A.G. Thosar (2013). Mathematical modelling and simulation of Permanent Magnet Synchronous Machine. *International Journal of Electronics and Electrical Engineering*, **1-2**: 66-71.
- Nayar, C., Tang, M. and W. Suponthana (2008). Wind/PV/Diesel Micro Grid System implemented in Remote Islands in the Republic of Maldives. IEEE International Conference Sustainable Energy Technologies, 1076-1080.
- Nithya, K. and M. Ramasamy (2014). Multi-Input DC-DC Converter for Renewable Energy Sources. *International Journal of Research in Engineering and Technology*, **3**: 7714-7719.
- Özbay, E. and M. Tunay (2010). Load Frequency Control for Small Hydro Power Plants Using Adaptive Fuzzy Controller. IEEE International Conference on Systems Man and Cybernetics, 4217-4223.
- Ozdemir, M. and A. Orhan (2012). The Application of Fuzzy Adaptive PI Control for Micro Hydro Power Plants. International Conference on Communications and Information Technology, 745-750.
- Sarker, K., Chatterjee, D. and S.K. Goswami (2014). An optimized co-ordinated approach for harmonic minimization of Doubly Fed Induction Generator connected micro-grid system. *Electrical Power and Energy Systems*, **64**: 58-70.
- Singh, Abinash and Balwinder Singh Surjan (2014). Microgrid: A review. *International Journal of Research in Engineering and Technology*, **3-2**: 185-198.
- Singh, S., Singh, A.K. and S. Chanana (2012). Operation and Control of a Hybrid Photovoltaic-Diesel-Fuel Cell System Connected to Micro-Grid. IEEE Power India Conference, 1-6.
- Soni, Y.K. and R. Bhatt (2013). BF-PSO optimized PID Controller design using ISE, IAE, IATE and MSE error criteria. *International Journal of Advanced Research in Computer Engineering & Technology*, **2-7**: 2333-2336.
- Suresh, M. and S.T. Srinivas (2013). Power Quality Improvement in Renewable Energy Interconnection Grid at Distribution Level. *International Journal of Engineering Research & Technology*, **2-10**: 83-89.
- Syed, M.H., Zeineldin, H.H. and M.S. El Moursi (2013). Grid Code Violation during Fault Triggered Islanding of Hybrid Micro-grid. IEEE Conference on Innovative Smart Grid Technologies, 1-6.
- Tenti, P., Costabeber, A., Trombetti, D. and Paolo Mattavelli (2010). Plug & Play Operation of Distributed Energy Resources in Micro-Grids. IEEE International Telecommunication Energy Conference, 1-6.

## Appendix

### System Parameters

Parameter	Value
Frequency	50Hz
Main grid voltage & Bus voltage	400V
Hydro subsystem data	<b>Synchronous machine</b> KVA rating 250 KVA Rated speed 1500 rpm Frequency 50 Hz Voltage 400 V
Wind subsystem data	<b>Asynchronous machine</b> HP or KW rating 160 KW (215 HP) Rated speed 1487 rpm Frequency 50 Hz Voltage 400 V
Solar subsystem data	<b>Wind turbine</b> Pitch angle 18 degrees Wind speed 12 m/s Short circuit current 7.34 A Open circuit voltage 0.6 V
Load	75 KW (2 nos.)



## Contents

<i>Editorial</i>	i
❑ <i>Snapshots</i>	ii
Pollution Charges and Assimilation Capacity in Tanjungpinang Bay Area, Riau Islands Province, Indonesia	
<i>Febrianti Lestari</i>	1
Impact on the Sardine Industries: Closed Fishing Season Policy, Zamboanga Peninsula, The Philippines	
<i>Teresita A. Narvaez, Bing Baltazar C. Brillo, Nizam D. Cornelio and Agnes C. Rola</i>	9
Removal of Aluminum(III) from Polluted Water Using Active Carbon Derived from Barks of <i>Ficus Racemosa</i> Plant	
<i>Anna Aruna Kumari and K. Ravindhranath</i>	23
Groundwater Quality Assessment through Water Quality Index (WQI) in New Karachi Town, Karachi, Pakistan	
<i>Adnan Khan and Faiza Riaz Qureshi</i>	41
GIS-based River Flood Hazard Mapping in Rural Area: A Case Study in Dabong, Kelantan, Peninsular Malaysia	
<i>Wani Sofia Udin, Nurul Asyikin Binti Ismail, Arham Muchtar Achmad Bahar and Mohammad Muqtada Ali Khan</i>	47
Comparison of Different Artificial Neural Networks Techniques and Autoregressive Models for Forecasting of PM <sub>10</sub>	
<i>Vibha Yadav and Satyendra Nath</i>	57
Urbanization and Its Effects on Water Resources: An Exploratory Analysis	
<i>Muhammad Abo ul Hassan Rashid, Malik Maliha Manzoor and Sana Mukhtar</i>	67
A Hydrological Tank Model Assessing Historical Runoff Variation in the Hieu River Basin	
<i>Ho Thi Phuong, Nguyen Xuan Tien, Hidetaka Chikamori and Kenji Okubo</i>	75
An Investigation on the Optimum Composition of Suitable Co-composting Material for the Enhancement of the Soil Organic Carbon in Mango Orchards of Pollachi, Tamil Nadu	
<i>N. Natarajan, K.R. Sabadini, R. Shunmuga Priya, A. Anbarasan and V. Sankar</i>	87
Determination of the Bioconcentration of Methidathion and Phosalone in Zebrafish ( <i>Brachydanio rerio</i> )	
<i>Byung Hyun Kim, Joon-Shik Moon, Chun-Geun Cha and Hun-Kyun Bae</i>	93
Use of Coir Pith as a Soil Amendment Material	
<i>C.R. Sahoo and B.B. Kar</i>	97
<i>Environment News Futures</i>	101